Evaluation of several conditioning matrices for the management of radioactive metal beryllium wastes

Pauline Bouhier, Céline Cannes, David Lambertin, Christian Grisolia, Davide Rodrigues, Sylvie Delpech

Evaluation of several conditioning matrices for the management of radioactive metal beryllium wastes

Pauline Bouhier,[1,2] Céline Cannes,[1,*] David Lambertin,[2] Christian Grisolia,[3] Davide Rodrigues,[1] Sylvie Delpech[1]

1 Université Paris-Saclay, CNRS/IN2P3, IJCLab, 91405 Orsay, France

2 CEA, DES, ISEC, DE2D, SEAD, Université de Montpellier, Bagnols-sur-Cèze, France

3 CEA, IRFM, Saint Paul-lez-Durance, France.

Keywords

Beryllium, corrosion, conditioning matrices, thermodynamic data, electrochemical measurements.

Abstract

Metal beryllium wastes are produced by nuclear industry. One way to manage them is their encapsulation in cements. The main risk of this conditioning is the aqueous corrosion, which leads to the hydrogen production and cracks causing a loss of radioactivity confinement. The corrosion can be limited by the formation of the hydroxide solid phase $Be(OH)_{2\,(s)}$. The stability domain of this phase was calculated in water as a function of the pH with a thermodynamic approach. M. Pourbaix has calculated a stability domain of $Be(OH)_{2(s)}$ from 2.9 to 11.7 for a total beryllium concentration of 10^{-4} mol.L^{-1}, while according to our calculation with more recent thermodynamic data, it is stable from 5.3 to 13.5. Thus, based on Pourbaix results, beryllium cannot be conditioned in the mainly used cement for nuclear waste, the ordinary Portland cement, while it is possible according to our calculations. Then, experimental measurements were done in order to select the data set most in agreement with the experimental observations. The beryllium reactivity has been examined in matrices having different pH pore solution: brushite cement (pH 1.75 - 6.44), magnesium phosphate cement (pH 5.6 - 8.4), calcium-sulfoaluminate (pH 10.9 - 12.3), Portland cement (pH 12.5 - 12.9) and activated slag (pH 12.9 - 13.8). The beryllium chemical behavior was

studied by measuring the open circuit potential and by electrochemical impedance spectroscopy. The experimental results are in agreement with the more recent thermodynamic data . Beryllium corrosion is too high in the brushite cement, leading to a high hydrogen production. This matrix can then not be envisaged for the conditioning of Be waste. If the beryllium is encapsulated in the activated slag, the highly alkalinity is too high in the early age, leading to a high aqueous corrosion. Activated slag are also not suitable for Be conditioning. The main conclusion of this paper is that beryllium can be encapsulated in safe conditions in the Portland cement, the magnesium phosphate cement and the calcium sulfoaluminate cement.

1. Introduction

Beryllium (Be) presents interesting properties, such as a low density, a relatively high melting point (1287 °C), a low neutron-capture cross section and a high neutron scattering cross section, a high specific heat and thermal conductivity, good mechanical properties at elevated temperatures and high oxygen gettering characteristics [1]. It is then employed in a wide range of applications and especially in nuclear industry. Be metal is currently employed in thermal reactors as a moderator, a reflector or fuel cladding [2-5]. It is also under study as interesting material for the future fusion power reactors. In the International Thermonuclear Experimental Reactor, Be constitutes the main plasma facing for the first wall of the tokamak and the neutron multiplier in the breeding blanket [6-10].

The use of beryllium in fission and fusion reactors will make it radioactive by neutron irradiation. Activated Be wastes will then be generated. Although some of the wastes can be cleared or recycled, it will remain large volume of metallic Be waste to consider. Depending on the dose rate, a near-surface or geological disposal can be proposed. Concrete encapsulation is one strategy to manage the low-and intermediate-level radioactive metallic wastes by isolating them from the environment [11-13]. It consists on the immobilization of the metal in a cementitious matrix. However, to ensure a safety storage, it is primordial to determine the reactivity of beryllium in the matrix and in the disposal environment. The literature on the radioactive beryllium waste management is really scarce. One reference considers four methods to condition the beryllium waste: cementation, bituminisation, vitrification and phosphatisation [14]. The authors concluded that phosphate and glass matrices would be the optimal solution to manage the beryllium waste. However, for cementation, they have only considered ordinary Portland cement as conditioning

matrix and they have assumed from literature data that the beryllium corrosion rate would be too high according to the pH of the pore water solution (higher than 12). However, recent experimental data have shown strong uptake of beryllium in ordinary Portland cement, low-pH cements and calcium-silicate hydrated cements, showing that these types of cement could be used as matrices for Be(II) conditioning [15, 16]. This uptake is controlled by sorption processes in the cement solid phases and the solubility has been found not relevant in the studied conditions.

However, the behavior of a metal in a conditioning matrix is mainly governed by its corrosion. Indeed, the major risk is the oxidation of the metal by the interstitial water, resulting in the hydrogen release. This can lead to gas driven transport of radionuclides out of the waste package. The confinement is no longer ensured. Beryllium presents a serious drawback, a very high toxicity. Beryllium in powder form is known as carcinogen and it can cause an incurable respiratory disease, the berylliosis [17, 18]. This may explain the few works on the chemistry of this element. Corrosion studies are nevertheless reported in the literature [19-25] which show that beryllium is highly corrosion resistant in water at low temperature. Moreover, studies have also shown that impurities in the surface can cause local corrosion [26] and the presence of aggressive anions in solution, such as chloride ions, can generate pitting corrosion [27-30]. The metal is protected by a layer of oxide $BeO_{(s)}$ or hydroxide solid phase $Be(OH)_{2\,(s)}$ of 20 to 100 angstroms thickness, when exposed to air. The reactivity of beryllium is mainly related to the stability of this protective layer. In acid solutions, the dissolution of the solid oxide layer is extensively proven, leading to a continuous corrosion of the metal. By contrast, in alkaline to hyperalkaline solutions, the studies on the solubility of the beryllium oxide or hydroxide solid phase are more controversial. While oldest studies based on thermodynamic calculation predict in alkaline solution the formation of anionic species, such as $Be_2O_3^{2-}$ [31], more recent studies show that the predominant species in alkaline to hyperalkaline (NaOH 5 $mol.L^{-1}$) solution are $Be(OH)_2$, $Be(OH)^{3-}$ and $Be(OH)_4^{2-}$ [32]. As anionic species have been formed in alkaline media, beryllium is not protected against the corrosion by a passivation phase. In such conditions, the corrosion is continuous. Although some studies have shown a strong uptake of beryllium species in low and high alkaline cementitious matrices, the high beryllium corrosion leads to a continuous production of hydrogen gas, which can compromise the nuclear waste confinement [15, 16].

We have undertaken a study on the reactivity of metal beryllium in conditioning matrices to propose the safest storage of the radioactivepackages containing beryllium waste. This study is

mainly based on (i) the exploitation of thermodynamic data reported in the literature, concerning the potential – pH diagram of beryllium in water to predict its corrosion behavior in cementitious matrices and (ii) the electrochemical measurements carried out on beryllium incorporated in a cement as a function of time and cement formulations. Five types of cement have been selected with pore water solution presenting different pH ranges: brushite cement, magnesium phosphate cement, calcium sulfoaluminate cement, ordinary Portland cement and activated slag. Two techniques have been selected: monitoring the open circuit potential (OCP) with time and electrochemical impedance spectroscopy (EIS) at OCP.

2. Experimental section

2.1. Chemical products and cement preparation

The activated slag (AS) was prepared by mixing 95 wt% of slag (from Ecocem) and 5 wt% of a 2.5 M NaOH solution.

The ordinary Portland cement (OPC) grade CEM I 52.5 PM-ES was selected. It is a low alkali cement with low tricalcium aluminate content.

The calcium sulfoaluminate cement (CSA) was prepared by mixing 80 wt% of calcium sulfoaluminate clinker with 20 wt% of anhydrite.

Magnesium phosphate cement (MPC) was prepared in a Turbula blender by mixing “hard-burnt” magnesium oxide, potassium dihydrogen phosphate, fly ash, and boric acid for 20 minutes in the following proportions (wt%): MgO: 7.62; KH_2PO_4: 25.71; fly ash: 33.33; sand: 33.33 H_3BO_3: 2.

The brushite cement was a commercial binder (FOTIMINE, from Sulitec) comprising a Fotimine powder A (wollastonite $CaSiO_3$ (98.4%) and calcite $CaCO_3$ (1.6%)) and a Fotimine solution B (phosphoric acid (9.3 ± 0.5 mol.L^{-1}, borax $Na_2B_4O_7$ (0.15 ± 0.01 mol.L^{-1}) to be mixed in the 1.25/1 mass ratio.

The characteristics of the types of cement are reported in the Table 1.

When cements consisted of a powder mixture, they were mixed in a Turbula blender for 20 minutes. Cement paste volumes of about 100 mL were prepared with a three bladed propeller stirrer according to the following protocol:

1) start with demineralized water,

2) add premixed powders while stirring at low speed (≈100 rpm) and
3) mix for 2 minutes at middle speed (≈600 rpm).
4) mix for 3 minutes at high speed (≈1200 rpm).

The paste water content was adjusted as necessary according to the types of cement; the cements differed by their fineness and chemical water demand (Table 2).

2.2. Cement pH measurements

The pH measurements were carried out with a Consort C3010 pH meter and a Mettler Toledo Inlab Expert Pt1000 pH probe. Calibration was performed with IUPAC pH standard solutions 1.679 – 4.005 – 6.865 – 10.012 and 12.45 (± 0.01).

The pore fluid pH of cement was carried out according to the protocol set up by Alonso et al. [32]: 300g of cements were prepared and divided into samples of approximately 30 g in tightly closed 50 mL vials. Samples were stored at room temperature (21 °C ± 1 °C) over a period of 30 minutes to 28 days. At each measurement deadline, a sample was ground (Ø < 1 mm), weighed precisely and suspended in demineralized water with a mass ratio of cement/water of 1. The sample is then stirred for 5 minutes before measuring the pH of the suspension. For the activated slag cement, a mass dilution of 100 of the suspension in demineralized water was performed to measure a pH within the calibration range of the pH meter.

2.3. Electrochemical measurements

A three-electrode cell was used for the electrochemical measurements, with a working electrode (beryllium wire), a counter electrode (platinum wire) and a quasi-reference electrode (platinum wire). The electrochemical set-up is reported in the Figure 1. The potential of the Pt wire was measured in solution, against a Ag/AgCl reference electrode, and was calculated against a normal hydrogen electrode (NHE) as a function of the pH (Figure 2). All potentials presented in this manuscript were calculated with respect to the NHE.

The beryllium wire (1.2 mm diameter, Goodfellow, purity 99.7%) was cut at different lengths. The surface of the Be electrodes was 1.17 cm^2 in the brushite cement, 0.98 cm^2 in the magnesium phosphate cement, 1.13 cm^2 in the calcium-sulfo aluminate cement, 1.21 cm^2 in the ordinary

Portland cement and 1.24 cm^2 in the activated slag. The Be wires were introduced in small pipette tip and maintained with a rapid glue (Araldite). The so-prepared Be electrodes were cleaned by rinsing them with ethanol and were pickled with a HCl (0.5 M) solution until a light grey appearance (around 1 min). Then they were rinsed thoroughly with demineralized water and dried with a tissue paper.

The Pt wire (diameter: 1 mm, Goodfellow, purity 99.9%) was cut to obtain in the electrochemical set-up an electrode surface of 1.26 cm^2. The wire was cleaned with ethanol and heated until bright-red color with a blowtorch.

As beryllium powder is highly toxic, the Be wire is stored and handled under a glove box, in case of formation of powder during its handling. The electrochemical experiments were carried out in this glove box. Just after their preparation, the cement pastes were transferred to plastic pots, which were immediately closed with the cap containing the electrodes. The five electrochemical cells were then stored in the glove box during all the measurement. The curing conditions are then: ambient temperature and under air. Previous experiments have shown that with this kind of set-up, the diffusion of the ambient atmosphere is very limited. No carbonation of samples is expected.

Measurements were carried out using a potentiostat (AMETEK model VersaSTAT 4) piloted by the VersaStudio software. Electrochemical Impedance Spectroscopy (EIS) diagrams were recorded at the open circuit potential with 10 mV amplitude. Frequency ranged between 10^5 and 10^{-1} Hz, with 10 frequencies values per logarithmic decade.

3. Results and discussion

3.1. Thermodynamic data

The reactivity of an element can be evaluated by a thermodynamic approach. For example, the potential-pH diagrams of one element in a given media, calculated from the thermochemical data of all the different chemical forms of this element , are used to determine its speciation in this media. From these diagrams, in the case of a metallic element, three potential-acidity zones can be defined corresponding to the immunity, the passivation and the corrosion domain of the element. The immunity zone corresponds to the stability domain of element in its metal state. In the corrosion zone, the metal is continuously oxidized to an ionic species. In the passivation zone, the

metal is oxidized to a solid phase, which can protect the metal and limit the corrosion reaction depending on the characterization of this solid phase: adherence, compacity, porosity, solubility. In general, in aqueous solution, the metal oxide or hydroxide phases allow a good protection against the corrosion for numerous metallic compounds.

Concerning beryllium, a first potential-pH diagram was calculated in water at 25°C by M. Pourbaix in 1963 [31] using the thermodynamic data of W.M. Latimer [34] (Fig. 3). Pourbaix has considered the solid phases Be, $Be(OH)_2$ amorphous, $Be(OH)_{2\ \alpha}$, $Be(OH)_{2\ \beta}$ and BeO and the soluble species Be^{2+}, Be_2O^{2+}, $Be_2O_3^{2-}$ and BeO_2^{2-}. The stability domain of the water is limited by its oxidation (O_2/H_2O) and its reduction (H_2O/H_2).

Figure 3 shows that Be is oxidized to Be(II) in water whatever the potential and the pH. In acidic media, for pH lower than 3, the stable form of beryllium is the soluble ionic species Be^{2+}. In highly alkaline solutions, the predominant form is $Be_2O_3^{2-}$. The diagrams were calculated for several concentrations of Be(II), 10^{-6}, 10^{-4} and 10^{-2}M.. In the case of beryllium, the passivation zone is expected to correspond to the stability domain of $Be(OH)_2$: pH from 3.9 to 10.7 for [Be(II)] = 10^{-6} M, pH from 2.9 to 11.7 for [Be(II)] = 10^{-4} M and pH from 1.9 to 12.7 for [Be(II)] = 10^{-2} M. In this pH range, the beryllium corrosion depends on the stability of the hydroxide layer. Pourbaix [31]The author has specified that the amorphous hydroxide is not stable in contact with air and water. It crystallizes in alpha and beta phase. The α-phase is metastable and gradually turns into β-phase, which is the most stable hydroxide phase considering the thermodynamic data.

The solubility of the hydroxide solid forms as a function of the pH was also calculated in the reference [31]. Differences between the solubility values calculated with the thermodynamic data and the values experimentally obtained were observed. The authors have attributed this discrepancy to an inaccuracy of the values of the free enthalpy of formation for the beryllium species.

However, no modification of the thermochemical data of Be(II) species is observed between 1965 and 1998, in the different reports from the National Institute of Standards and Technology [35-37]. The main difference between the thermochemical data in these reports and the ones given by Latimer is the absence of data for $Be_2O_3^{2-}$, which was the predominant species in the highest pH zone of the diagram calculated by Pourbaix. Studies on the hydrolysis of beryllium confirm the formation of monomeric species such as $Be(OH)_{2\ \alpha}$, $Be(OH)_{2\ \beta}$, $Be(OH)_{2\ aq}$ and show the stability

of polynuclear ones such as $Be_2(OH)^{3+}$, $Be_3(OH)_3^{3+}$, $Be_5(OH)_6^{4+}$ and $Be_6(OH)_8^{4+}$ for concentrations of Be(II) in solution higher than 10^{-4} mol.L^{-1} [38, 39]. The associated constants of formation of these species have also been reported. In 2016, all the thermodynamic data on the speciation and hydrolysis of Be in aqueous solution have been published in the reference [39] without considering $Be(OH)_4^{2-}$. Very recently, an experimental study on the solubility of beryllium species has been carried out in acidic to hyperalkaline solutions to accumulate thermodynamic data on beryllium [32].

Based on the thermodynamic data reported in the literature [32, 39, 40, 41], we have calculated the E-pH diagram of beryllium for a concentration of 10^{-6}, 10^{-4} and 10^{-2} mol.L^{-1} at 25°C considering the following species: Be, Be^{2+}, $BeOH^+$, $Be(OH)_{2\alpha}$, $Be(OH)_3^-$, $Be(OH)_4^{2-}$, $Be_2(OH)^{3+}$, $Be_3(OH)_3^{3+}$, $Be_5(OH)_6^{4+}$ and $Be_6(OH)_8^{4+}$. The hydroxide solid phase $Be(OH)_{2\ \alpha}$ has been considered and not $Be(OH)_{2\,\beta}$ because the form α has been shown as the most experimentally stable phase at room temperature [32]. The diagrams calculated using the thermodynamic data of the references [32, 39, 40, 41] are given Figure 4. The considered acido-basic reactions and the electrochemical reactions to draw the diagrams with the associated thermodynamic data are reported respectively in the Tables 3 and 4. The diagram calculated at a beryllium concentration of 10^{-6} M (Fig. 4) is very different to the one calculated by Pourbaix (Fig. 3). The cationic species $Be(OH)^+$ is the predominant species at pH from 5.4 to 7.2 and in the alkaline domain, two species are stable, $Be(OH)_3^-$, from 11.7 to 13.3 and $Be(OH)_4^{2-}$, from pH 13.3 to 16. The diagrams calculated at a concentration of 10^{-4} and 10^{-2} M present the same predominant species: Be^{2+}, $Be(OH)_2$ and $Be(OH)_4^{2-}$. We can also observe a very short domain of stability for the species $Be_3(OH)_3^{3+}$ at 10^{-2} M, from pH 4.28 to 4.32. At these concentrations, the diagrams calculated by Pourbaix and the ones calculated in this work differs mainly in the alkaline to hyper-alkaline region: the stable chemical form of beryllium is $Be(OH)_4^{2-}$.instead of $Be_2O_3^{2-\ -}$.

Moreover, the main difference of these diagrams compared with the diagram calculated by Pourbaix [31] is a shift of the passivation domain towards the highest pH values: 7.2-11.7 at 10^{-6} M ; 5.3-13.5 at 10^{-4} M ; 4.3-14.5 at 10^{-2} M.. This pH shift is explained by (i) considering the α instead of β phase for $Be(OH)_2$ and (ii) the absence of thermochemical data for $Be_2O_3^{2-}$ in the recent databases.

3.2. Selection of conditioning matrices

The ordinary Portland cement (OPC) presents several intrinsic qualities: availability, low cost, ease of use, good mechanical strength and, in general, stability over time. The basicity of hydrated Portland cement is an advantage in the field of radioactive waste because this material is capable of insolubilizing a large number of radionuclides (generally conditioned at high oxidation states) [42, 43]. Therefore, OPC is the mainly used matrix for conditioning low- or intermediate-level waste. However, this basicity can present an obstacle for conditioning reactive metals, which are oxidized in a soluble species in this alkaline pH domain with production of hydrogen gas. Five types of cement have then been selected with different pore solution pH, to determine the best matrix for beryllium waste conditioning: activated slag (AS), ordinary Portland cement (OPC), calcium-sulfoaluminate cement (CSA), magnesium phosphate cement (MPC) and brushite cement (BC).

The pH of these cements has been measured as a function of time (Figure 5). The reactivity of beryllium can be studied on the entire pH domain, since the brushite cement presents an acid pore solution (pH from 1.75 to 6.44), the magnesium phosphate cement a neutral pore solution (pH from 5.6 to 8.4), the calcium-sulfoaluminate has a basic interstitial solution (pH from 10.9 to 12.3), the Ordinary Portland cement is highly alkaline (pH from 12.5 and 12.9) and the pH values are the highest for the activated slag (from 12.9 to 13.8).

The beryllium corrosion depends strongly on the characteristic of the hydroxide solid phase: solubility, adherence, porosity, compacity. According to the thermodynamic data, two stability domains have been determined for this solid phase.. The pH domains of the selected cements have been superimposed to the stability domain of the hydroxide phase determined with the thermodynamic data at the three different concentrations. Two different chemical behavior are expected from the Figure 6.

The pH solution will also be modified by the corrosion reaction. When Be^{2+} is oxidized by water, the reaction produces H_2 but also OH^- ions, which increases the pH of the pore solution. On the other hand, when anions are produced in high pH domain, the oxidation reaction consumes OH^-, thus decreases the pH of the solution. In all cases, the tendency is to go to the stability domain of the beryllium hydroxide solid form. The influence of corrosion reaction on pH solution will depend on the amount of metal against the volume of matrix. In the frame of this study, the ratio (cement

volume) / (metal volume) is close to 5000. Thus, we can consider that the variation of pH is only monitored by the cement setting.

If we consider the Pourbaix work, in the activated slag and the ordinary Portland cement, the hydroxide solid layer should be dissolved in the ionic species $Be_2O_3^{2-}$. A continuous aqueous corrosion of Be is therefore expected with production of hydrogen. In the calcium-sulfoaluminate cement, a corrosion should be observed during the first days of immersion and should progressively be diminished since the pH of this type of cement tends to 10.9, a value ranging in the pH domain of $Be(OH)_2$ stabilityf. The corrosion of beryllium to the soluble Be^{2+} species is expected in the brushite cement during the first day. However, the corrosion should be quickly limited by the formation of the hydroxide solid phase $Be(OH)_2$. Finally, the magnesium phosphate cement is the only one with pore solution pH values in the domain of stability of the protective layer. The Be reactivity should be the lowest in this type of cement.

According to our calculations, three types of cement, OPC, CSA and MPC, present pore solution pH values ranging in the domain of the stability of the hydroxide solid $Be(OH)_2$. Under these conditions, beryllium should be protected against the corrosion and these three types of cement could be selected as conditioning matrices for beryllium waste. Activated slag presents a mitigate case, as the pH values of its interstitial solution is too high during the first days. The predominant form of beryllium should be the soluble species $Be(OH)_3^-$ or $Be(OH)_4^{2-}$. A corrosion should then take place in this type of cement during the first days of encapsulation. BC can definitively not be chosen for conditioning of beryllium wastes. According to the last thermodynamic data, the pH of this cement is too acid. Beryllium should be corroded in the Be^{2+} soluble species with production of hydrogen during several days.

This study put in evidence two different chemical behaviors of beryllium taking into account the thermodynamic data. It is then important to perform experimental measurements on the Be reactivity in the different types of cement to be able to propose a safe confinement for this nuclear waste.

3.3. Electrochemical measurements of Be in conditioning matrices

The reactivity of Be has been studied using the same electrochemical approach that the one adopted previously to study the reactivity of Al and U encapsulated in a conditioning matrix: open circuit potential and electrochemical impedance spectroscopy measurements [44-46].

OCP measurements

The open circuit potential (or the potential at zero current) characterizes the redox reaction involved at the electrode interface. It depends on the nature of the oxidizing agent and on the reaction kinetic. In the case of an aqueous corrosion, the potential is close to the reduction potential of water and if the metal is protected against the corrosion, the OCP tends to increase. The greater the difference between the OCP and the reduction potential of water, the less corroded the metal. The OCP measurement can then indicate qualitatively the reactivity of the metal at any hydration time of the cement.

The variation of the beryllium OCP encapsulated in a matrix has been measured as a function of time (in day) for the five types of cement. As a usual reference electrode cannot be used in a cement, a platinum pseudo-reference has been selected for the electrochemical measurements. The calibration curve, potential of platinum against the normal hydrogen electrode (NHE) as a function of the pH, given in the experimental section (Fig. 2), has been used to calculate the potential of beryllium against the normal hydrogen electrode. Knowing the evolution of the pH of the interstitial solution of the cement, the Pt potential can be calculated for each measurement and the OCP measured on beryllium electrode can be given against the NHE reference electrode.

Figure 7 shows that for all the types of cement, OCP first increases and tends to a plateau. The OCP is the highest in the Portland cement, while it is the lowest in the activated slag during the first days of immersion. The increasing period of OCP and the constant values obtained at the end of the studied periods depend on the type of cement. After more than 100 days of immersion, the OCP is the highest in the magnesium phosphate cement and the lowest in the activated slag. The measurements on Be electrode in the brushite cement have been stopped after one month, because it was difficult to acquire electrochemical data with high quality. This has been attributed to the high production of hydrogen at the Be surface by aqueous corrosion in this acid cement. The electrode/medium is perturbed by the formation of this gas. Large bubbles have been observed in the vicinity of the beryllium electrode. Nevertheless, we cannot conclude on the reactivity of beryllium in the selected cements by comparing directly the variation of the OCP as a function of time for each type of cement. The reduction potential of water depends on the pH, which varies both as a function of the type of cement and time. In order to compare Be(II)/Be and H_2O/H_2 redox

potentials, the theoretical potential of the redox couple H_2O/H_2 has been calculated by applying the Nernst equation at the measured pH of the cement at a given time ($E_{H2O/H2}$ /ENH = 0 - 0.059 pH). The values are reported Figure 7 and compared to the Be OCP ones for each type of cement.

The main observations are:

- At long term, in the Portland cement and in the calcium sulfoaluminate cement, the variations of Be OCP and H_2O/H_2 redox potential are similar. The difference between the two values is close to 0.8 V (Fig. 8). This result shows a very low corrosion of Be during all the immersion time. In these two types of cement, Be is in passivation conditions. The metal is protected by a stable layer formed on its surface. That agrees with our thermodynamic calculations presented in this paper.

- During the first days, Be seems more reactive in CSA than in OPC since the OCP is just 0.26 V higher than the H_2O/H_2 redox potential (Fig. 8). In CSA, hydrogen is produced at the beginning of the conditioning.

- In magnesium phosphate cement, the variation of the Be OCP is not similar to the one observed in the Portland and the calcium sulfoaluminate cements. It takes more than 40 days instead of 7 days to observe a plateau for the OCP values. At long term, the difference Be OCP – E (H_2O/H_2) reaches 0.7 V (Fig. 8), which is quite high. We suppose that after about 40 days of immersion, a protective layer is formed at the Be surface ensuring efficient passivation. By contrast, the first day, the OCP value is just 0.18 V higher than the redox potential of water. This result suggests that at the beginning, beryllium is corroded if it is immersed in a magnesium phosphate cement. That can be explained by the low pH of this cement at the early age. The protective layer seems not stable in these conditions.

- In the activated slag, a plateau is observed for the OCP variation with time from 25 days. The maximal difference measured between the Be OCP and the H_2O/H_2 redox potential is 0.59 V (Fig. 8), which is lower than the values measured in the OPC, CSA and MPC. Moreover, as this difference reaches values around 0.3 and 0.4 V during the first days, we can assume that Be is corroded in this type of cement during this period.

- The worst case is observed when beryllium is encapsulated in the brushite cement. During the entire studied period, the OCP values are comparable to the H_2O/H_2 redox potential (Fig. 8). We conclude that beryllium is highly corroded in the brushite cement with production of high amount

of hydrogen. This production of gas has been confirmed by the formation of bubbles at the vicinity of the beryllium surface.

The OCP measurements are in good agreement with the results obtained by our thermodynamic calculation. Three types of cement can be retained for the Be waste conditioning: OPC, CSA and MPC, whereas the brushite cement is definitively not adequate. In BC, the Be corrosion is too high, leading to a too high production of hydrogen in the waste package. AS can also not be chosen for Be conditioning because of its aqueous corrosion during the first days of immersion.

EIS measurements

Electrochemical Impedance Spectroscopy is an interesting technique for understanding the reactivity of redox compounds and to access to data on the evolution of the interface metal/electrolyte with time. Moreover, if the EIS is recorded at the OCP, this technique presents the advantage not to alter the metal sample/medium interface. The reactivity of the metal can be examined *in situ* and during a long-time range. The electrochemical impedance spectra, in Nyquist and Bode representations, have been recorded on a beryllium electrode in the five types of cement. We have previously shown that cement brings an electrical contribution to the impedance measurement [45]. In order to discriminate the impedance related to the cement from the one related to the beryllium reactivity, measurements on a platinum electrode, as an inert electrode, have been performed in parallel.

Impedance is generally modelled with an electrical circuit (Figure 9). Two parts of the circuit have to be distinguished. The first part corresponds to the impedance contribution to the cement matrix (Z_{matrix}). The details of this impedance are already described in the reference [45]. Each matrix has its own impedance contribution. The second part corresponds to the impedance related to the electrochemical process involving at the metal/matrix interface. This impedance is constituted of the double layer capacitance (C_{dl}) or a constant phase element (CPE) [47] in parallel with the faradaic impedance (Z_{FAR}), which is characteristic of the electrochemical reactions involving at the electrode/media interface. When a passivation process occurs at the metal/matrix interface, the faradaic impedance tends to a very high value and the current flows through the capacitive branch (or CPE). That is called “capacitance effect” and the shape of the Nyquist diagram is close to a capacitance response, which means a linear variation parallel to the Z_i-axis.

- Cement contribution to EIS measurements

The EIS measurements realized on Pt electrode are given Figure 10. For all the matrices except CSA, the contribution of the cement involves at high frequencies between 10^5 and 10^3 Hz. In the case of CSA, the matrix contribution involves in the all frequency domain. That is particularly observed after 100 days with the apparition of a loop at high frequencies. This loop can be characteristic of (i) an electroactive species in the pore solution or (ii) an evolution of the porosity of the matrix.

- Be reactivity contribution to EIS measurements

Figure 11 and 12 present the evolution of EIS diagrams recorded respectively in the brushite cement and the four other types of cement on Be electrode as a function of time. Be spectra recorded in BC (Fig. 11) are not exploitable probably because of H_2 bubbles formation when Be is introduced in the matrix, which inhibits the electrical contact with the electrode and the potentiostat. The evolution with time of Be impedance recorded in OPC and MPC is low. In these two types of cement, a capacitive effect is observed on EIS spectra, corresponding to a passivation layer at the electrode surface. In AS, the impedance begins with a capacitive loop, which increases with time. That is explained by a passivation process, which occurs after 40 immersion days, probably in relation with the decrease of the cementitious matrix pH with time.

Measurements carried out on Be electrode in CSA present the same shape than the diagrams recorded on Pt electrode. It is not possible to separate the contribution of the matrix from the electrochemical process involved on Be electrode. No conclusion can be given from EIS spectra recorded in CSA. However, based on OCP measurements, it seems that Be is passivated in CSA during all the immersion period.

It is difficult to compare the reactivity of Be in OPC and MPC on the basis of a qualitative approach. The Bode diagrams present a frequency shift between these two types of cement. That can be due to the matrix contribution or to the double layer capacitance, which depends on the type of matrix. In both cases, a strong passivation process is observed. This passivation process is also observed in AS after 40 days. These observations are in agreement with the E-pH diagram calculated in this paper and with the evolution of the matrices pH with time.

Conclusion

Due to its specific properties, beryllium is a metal compound used in the nuclear industry. The management of Be nuclear waste has then to be considered. One way to manage the low- and intermediate-level waste is the encapsulation in a cement. To select the best matrices for beryllium waste conditioning, five types of cement, having pore solution with different pH, have been selected: activated slag, Portland cement, calcium sulfoaluminate cement, magnesium phosphate cement and brushite cement. The reactivity of beryllium has first been studied in water as a function of the pH, a key parameter, by using a theoretical approach. The beryllium data are relatively scarce. A potential-pH diagram has been established in 1963 by M. Pourbaix. According to these data, beryllium waste cannot be conditioned in highly alkaline solution, such as the pore solution of OPC, AS and CSA. If we consider only the pH parameter, a neutral medium such as the MPC seems the only cement capable of a safe conditioning of the beryllium waste. The evolution of the thermodynamic database and the recent published data have led us to re-calculate the E-pH diagram of Be which shows that Be is stable in neutral to highly alkaline solutions. Thus, the beryllium should be passivated by the hydroxide solid phase $Be(OH)_2$ in OPC, CSA and MPC, while its corrosion is too high in brushite cement and activated slag to envisage them as conditioning matrices. To confirm these first results, an electrochemical study, by measuring the open circuit potential and the electrochemical impedance, has also been undertaken to follow the reactivity of beryllium in the different types of cement with time. This study is carried out in situ and offers the advantage of considering several parameters and not only the pH, such as the charge transfer kinetic and the level of passivation of the solid layer. The experimental results confirm the behavior of beryllium expected by our thermodynamic calculations. A summary of these results is given Table 5.

The beryllium nuclear waste can be conditioned in a Portland cement, a calcium sulfoaluminate cement or a magnesium phosphate cement. However, in MPC a corrosion is observed during the first days, while in OPC the beryllium is highly passivated during the entire studied time range. In the activated slag, the corrosion of beryllium is higher than in OPC and CSA during an immersion of 40 days. The production of hydrogen by aqueous corrosion should be too high to propose the AS as a conditioning matrix for Be waste. Moreover, the experimental data confirm that the brushite cement has to be excluded to encapsulate the beryllium. It would be interesting to confirm

these results by measuring the volume of hydrogen gas produced in each type of cement by gas chromatography. This will be done in a future work.

Author information

Corresponding author: celine.cannes@ijclab.in2p3.fr / 33 1 69 15 71 52
IJCLab, Université Paris-Saclay, CNRS/IN2P3, 15 rue Georges Clémenceau, 91405 Orsay cedex, France

References

[1] K. A. Walsh, *Beryllium chemistry and processing*, 2009, ASM International.

[2] H. Pih, A survey of beryllium technology and nuclear applications, ORNL-4421 report 1969.

[3] J.M. Beeston, Nucl. Eng. Des. 14 (1970) 445-474.

[4] L.L. Snead, S.J. Zinkle, AIP Conference Proceeding 746 (2005) 768.

[5] D. Chandler, G.I. Maldonado, L.D. Proctor, R.T. Primm, Nucl. Tech. 177 (2012) 395-412.

[6] J.S. Park, X. Bonnin, R. Pitts, Nucl. Fusion 61 (2021) 016021-01636.

[7] J.H. Kim, S. Nakano, M. Nakamichi, J. Nucl. Mater. 542 (2020) 152522-152529.

[8] D.L. Smith, W. Daenner, G. Kalinin and H. Yoshida, J. Nucl. Mater. 179-181 (1991) 1185-1188.

[9] J.H. Kim, M. Nakamichi, J. Nucl. Mater. 453 (2014) 22-26.

[10] E. Pajuste, G. Kizane, I. Igaune, L. Avotina, Jet Contributors, Nucl. Mater. and Energy 19 (2019) 131–136.

[11] J. Li, J. Wang, J. Hazard. Mat. B 135 (2006) 443

[12] F. Glasser, *Application of inorganic cement to the conditioning and immobilisation of radioactive wastes*, in Handbook of advanced radioactive wastes conditioning technologies, p. 67-135 (2011).

[13] N.B. Milestone, Adv. Appl. Ceram. 105 (2006) 13

[14] F. Druyts, P. Van Iseghem, Fusion Eng. Des. 69 (2003) 607-610.

[15] B. Grambow, M. Lopez-Garcia, J. Olmeda, M. Grivé, N. C.M. Marty, S. Grangeon, F. Claret, S. Lange, G. Deissmann, M. Klinkenberg, D. Bosbach, G. Bucur, I. Florea, R. Dobrin, M. Isaacs, D. Read, J. Kittnerova, B. Drtinova, D. Vopalka, N. Cevirim-Papaioannou, N. Ait-Mouheb, X. Gaona, M. Altmaier, L. Nedyalkova, B. Lothenbach, J. Tits, C. Landesman, S. Rasamimanana, S. Ribet, Appl. Geochem. 112 (2020) 104480-104493.

[16] N. Cevirim-Papaioannou, I. Androniuk, S. Han, N. Ait Mouheb, S. Gaboreau, W. Um, X. Gaona, M. Altmaier, Chemosphere 282 (2021) 131094-131105.

[17] A. Seidler, U. Euler, J. Muller-Quernheim, K.I. Gaede, U. Latza, D. Groneberg, S. Letzel, Occup. Med. C 62 (2012) 506-513.

[18] S.D. Dai, G.A. Murphy, F. Crawford, D.G. Marck, M.T. Falta, P. Marrack, J.W. Kappler, A.P. Fontenot, Proc. Natl. Acad. Sci. 107 (2010) 7425-7430.

[19] V.D. Scott, G.V.T. Ranzetta, J. Nucl. Mater 9 (1963) 277-289.

[20] E.T. Shapovalov, V.V. Gerasimov, Soviet Atomic Energy 26 (1969) 498-502.
[21] E. Gulbrandsen, A.M.J. Johansen, Corr. Sci. 36 (1994) 1523-1536.
[22] M.A. Hill, D.P. Butt, R.S. Lillard, J. Electrochem. Soc. 145 (1998) 2799-2806.
[23] A. Venugopal, D.D. Macdonald, R. Varma, J. Electrochem. Soc. 147 (2000) 3673-3679
[24] F. Druyts, Fusion Eng. Des. 75-79 (2005) 1261-
[25] S. He, H. Ye, Y. Ma, L. Guo, Y. Gou, P. Zhang, Corr. Sci. 107 (2016) 21-30
[26] J.S. Punni, M.J. Cox, Corr. Sci. 52 (2010) 2535-2546.
[27] M.E. Straumanis, D.L. Mathis, J. Electrochem. Soc. 109 (1962) 434-436.
[28] K.G. Sheth, J.W. Johnson, W.J. James, Corr. Sci. 9 (1969) 135-144.
[29] R.U. Vaidya, M.A. Hill, M. Hawley, D.P. Butt, Metall. Mater. Tranns A 29A (1998) 2753-2760.
[30] R.S. Lillard, J. Electrochem. Soc. 148 (2001) B1-B11.
[31] M. Pourbaix, *Atlas d'équilibres électrochimiques*, Gauthier-Villars & Cie, Paris (1963).
[32] N. Çevirim-Papaioannou, X. Gaona, M. Böttle, E.Y. Bethune, D. Schild, C. Adam, T. Sittel, M. Altmaier, Appl. Geochem. 117 (2020) 104601-104612.
[33] M. C. Alonso et al., *Cement-Based Materials for Nuclear Waste Storage*, New York, NY: Springer New York, (2013), 251–259.
[34] W. M. Latimer, The Oxidation States of the Elements and Their Potentials in Aqueous Solutions. Prentice Hall Incorporated, 1952.
[35] V. B. Parker, D. D. Wagman, and W. H. Evans, "NBS Technical Note 270-6 - Selected Values of Chemical Thermodynamic Properties, Tables for the Alkaline Earth Elements (Elements 92 through 97 in the Standards Order of Arrangement)," 1971.
[36] D. D. Wagman, The NBS Tables of Chemical Thermodynamic Properties: Selected Values for Inorganic and C1 and C2 Organic Substances in SI Units. American Chemical Society and the American Institute of Physics for the National Bureau of Standards, 1982.
[37] M. Chase, "NIST-JANAF Thermochemical Tables, 4th Edition," Journal of Physical and Chemical Reference Data, Monograph 9, 1998.
[38] J. Bruno, J. Chem. Soc. Dalt. Trans., 10 (1987) 2431–2437.
[39] P. L. Brown and C. Ekberg, Eds., Hydrolysis of Metal Ions. Weinheim, Germany: Wiley-VCH Verlag GmbH & Co. KGaA, 2016.
[40] Thermodynamic Data for Fifty reference Elements, NASA-TP-3287, N93-19977, (1993)

[41] Shock E.,Sassani D.C.,Willis M.,Sverjensky D.A Inorganic species in geologic fluids: Correlations among standard molal properties of aqueous ions and hydroxide complexes. Geochim. Cosmochim. Acta 61 (1997) 907-951.
[42] N.B. Milestone, Adv. Appl. Ceram. 105 (2006) 13-20.
[43] M. Atkins, F.P. Glasser, Waste Management 12 (1992) 105-131.
[44] C. Cau Dit Coumes, D. Lambertin, H. Lahalle, P. Antonucci, C. Cannes, S. Delpech. J. Nucl. Mat. 453 (2014) 31-40.
[45] S. Delpech, C. Cannes, N. Barré, Q. Thuan Tran, H. Lahalle, D. Lambertin, S. Gauffinet, C. Cau Dit Coumes. J. Electrochem. Soc. 164 (2017) C717-C727.
[46] C. Cannes, D. Rodrigues, N. Barré, D. Lambertin, S. Delpech, J. Nucl. Mater. 518 (2019) 370-379.
[47] A.J. Bard, L. R. Faulkner, "Electrochemical methods: Fundamentals and applications", John Wiley and sons Ed., 2001, p375.

Table 1: Characteristics of the binder constituents.

	Supplier	**Constituents (wt%)**
Activated slag	Ecocem	CaO (43.0), SiO_2 (37.3), Al_2O_3 (10.7), MgO (6.5), S^{2-} (0.8), TiO_2 (0.7), Na_2O (0.68), K_2O (0.35), Fe_2O_3 (0.2), SO_3 (0.1), Cl^- (0.01)
Portland cement CEM I 52.5 PM-ES CP2	Lafarge (Le Teil)	$3CaO.SiO_2$ (65.6), $2CaO.SiO_2$ (16.0), $3CaO.Al_2O_3$ (4.0), $4CaO.Al_2O_3.Fe_2O_3$ (5.6), $CaCO_3$ (2.8), Gypsum (4.8)
Calcium sulfoaluminate clinker	Vicat	CaO (45.07), Al_2O_3 (23.46), SiO_2 (10.55), Fe_2O_3 (9.70), SO_3 (8.07), TiO_2 (1.29), MgO (1.00), K_2O (0.27)
Anhydrite (calcium sulfate)	Vicat	Purity ≥ 85%
Magnesium oxide, MgO MagChem 10CR	M.A.F. Magnesite	Purity ≥ 98.2%
Potassium dihydrogen phosphate, KH_2PO_4	VWR	Purity ≥ 98%
Boric acid, H_3BO_3	VWR	Purity ≥ 99.5%
Fly ash	EDF	Chemical composition (wt%): CaO (5.1%), SiO_2 (51.5%), Al_2O_3 (25.2%), Fe_2O_3 (5.8%), MgO (1.8%), Na_2O (0.4%), K_2O (1.3%), TiO_2 (1.3%), P_2O_5 (0.98%), SO_3 (0.66%)
Sand	Sobelco (Mios)	Granulometry < 1 mm

Table 2**:** Water content of cement pastes

Type of cement	Activated slag	Portland	Calcium sulfoaluminate cement	Magnesium phosphate cement	Brushite cement
w/*c*	0.50	0.40	0.55[a]	0.51[b]	1.25[c]

[a] water / (calcium sulfoaluminate clinker + gypsum); [b] water / ($MgO + KH_2PO_4$); [c] solution/cement

Table 3: Acido-basic reactions considered for the calculation of the E-pH diagram (presented Figure 4) with the values of the associated reaction constant (K) from [32, 39, 40, 41].

Acido-basic equilibrium	log K
$Be^{2+} + H_2O \leftrightarrow BeOH^+ + H^+$	-5.39
$Be^{2+} + 2H_2O \leftrightarrow \alpha\text{-}Be(OH)_2 + 2H^+$	-6.6
$2Be^{2+} + H_2O \leftrightarrow Be_2OH^{3+} + H^+$	-3.54
$3Be^{2+} + 3H_2O \leftrightarrow Be_3(OH)_3^{3+} + 3H^+$	-8.83
$5Be^{2+} + 6H_2O \leftrightarrow Be_5(OH)_6^{4+} + 6H^+$	-19.1
$6Be^{2+} + 8H_2O \leftrightarrow Be_6(OH)_8^{4+} + 8H^+$	-26.3
$Be^{2+} + 3H_2O \leftrightarrow Be(OH)_3^- + 3H^+$	-24.3
$Be^{2+} + 4H_2O \leftrightarrow Be(OH)_4^{2-} + 4H^+$	-37.6

Table 4: Electrochemical reactions considered for the calculation of the E-pH diagram (presented Figure 4) with the values of the associated reaction enthalpy (ΔG^0) from [32, 39, 40, 41] and of the standard potential (E^0).

Electrochemical reaction	Nernst Relation	ΔG^0 ($J.mol^{-1}$)	E^0 (V/NHE)
$Be^{2+} + 2e^- \rightarrow Be$	$E = E° + \frac{2.3RT}{2F}\log[Be^{2+}]$	378922	-1.96
$Be(OH)^+ + H^+ + 2e^- \rightarrow Be + H_2O$	$E = E° + \frac{2.3RT}{2F}\log[Be(OH)^+] - \frac{2.3RT}{2F}pH$	348207	-1.80
$Be(OH)_2(\alpha) + 2H^+ + 2e^- \rightarrow Be + 2H_2O$	$E = E° - \frac{2.3RT}{F}pH$	341312	-1.77
$Be(OH)_3^- + 3H^+ + 2e^- \rightarrow Be + 3H_2O$	$E = E° + \frac{2.3RT}{2F}\log[Be(OH)_3^-] - \frac{2.3RT}{2F}3pH$	240450	-1.25
$Be(OH)_4^{2-} + 4H^+ + 2e^- \rightarrow Be + 4H_2O$	$E = E° + \frac{2.3RT}{2F}\log[Be(OH)_4^{2-}] - \frac{2.3RT}{F}2pH$	164651	-0.85

Table 5: Summary of the passivation of Be expected from thermodynamic calculations, OCP and EIS measurements

	BC	MPC	CSA	OPC	AS
Thermo.	+	++	+++	+++	+
OCP	-	++	+++	+++	+
EIS	-	+++	non-usable data	+++	+

Figure 1: Electrochemical set-up for open circuit potential and electrochemical impedance spectroscopy measurements.

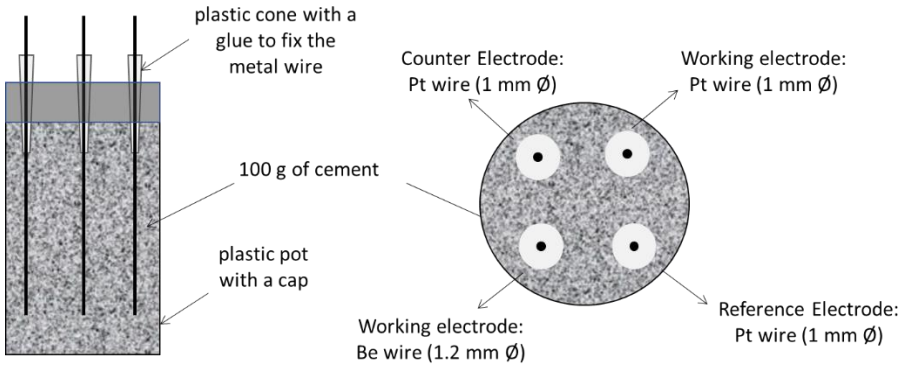

Figure 2: Variation of the platinum potential with the pH in aqueous solution.

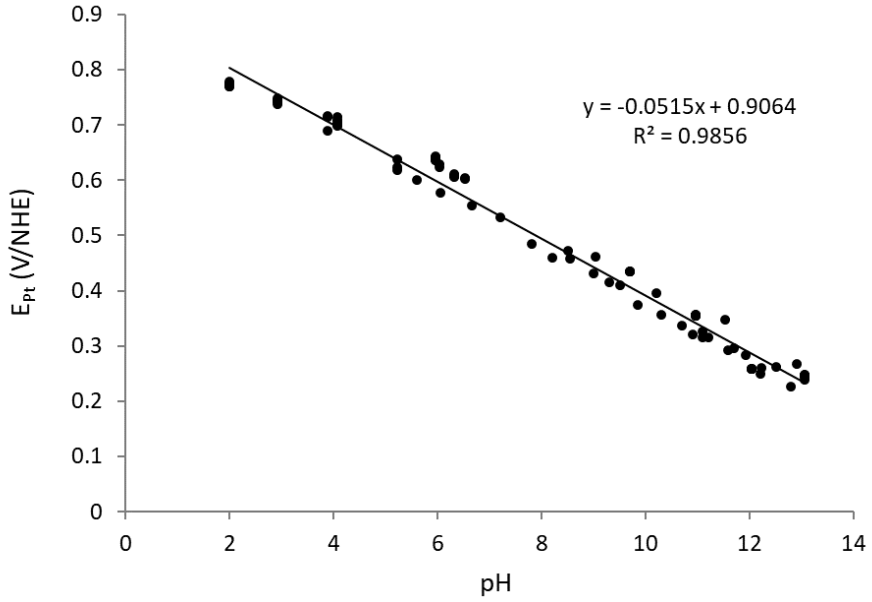

Figure 3: Potential – pH diagram of beryllium for 10^{-6} (− −), 10^{-4} (−−)and 10^{-2} (− •) mol.L^{-1} in water at 25°C, calculated by M. Pourbaix [31]

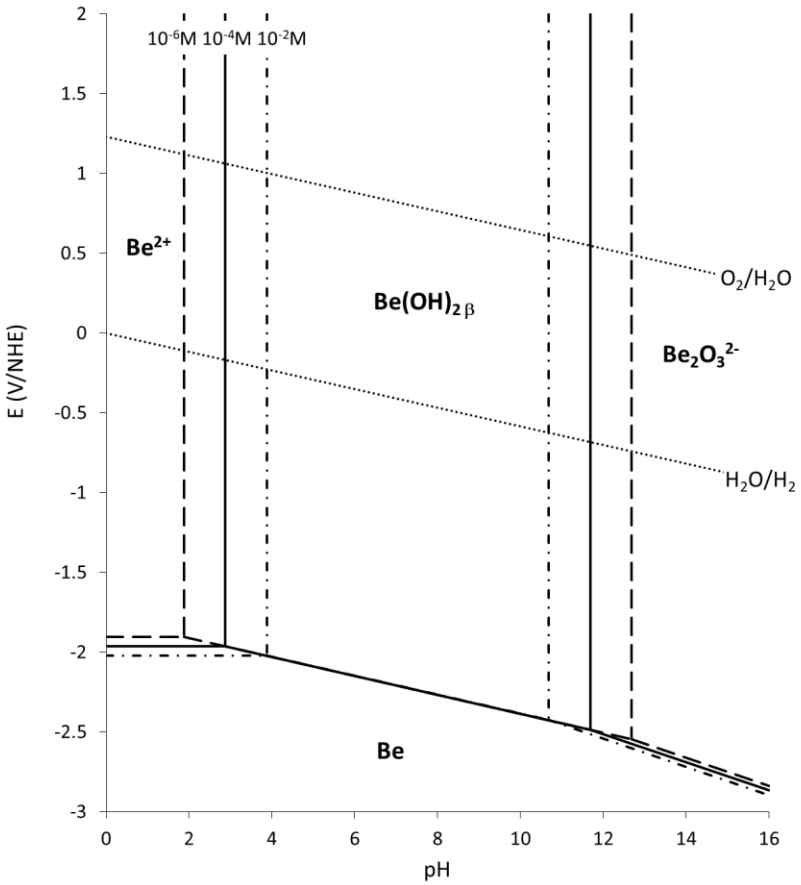

Figure 4: E – pH diagram of beryllium in water calculated for 10^{-6}, 10^{-4} and 10^{-2} mol.L^{-1} at 25°C in this work.

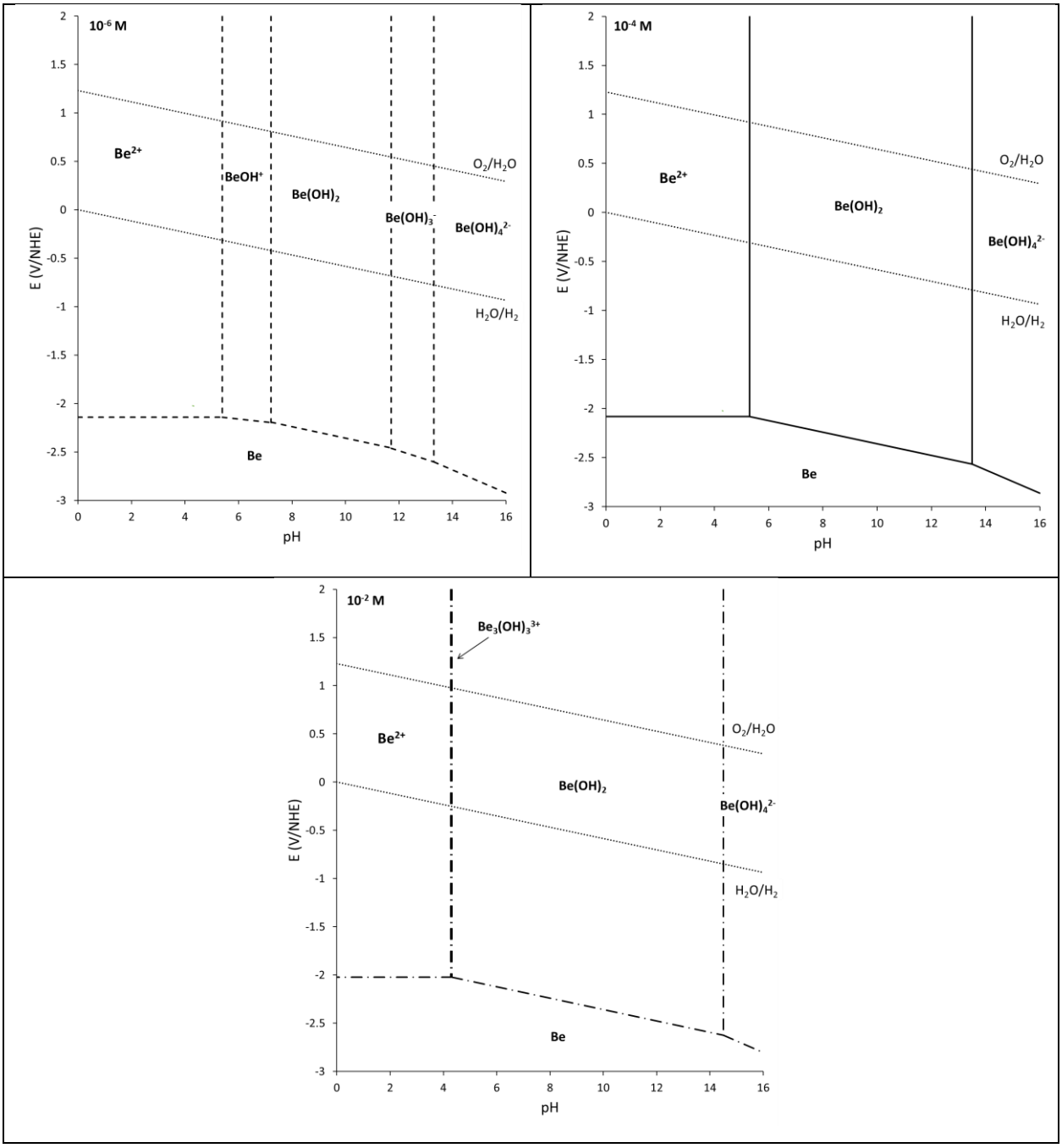

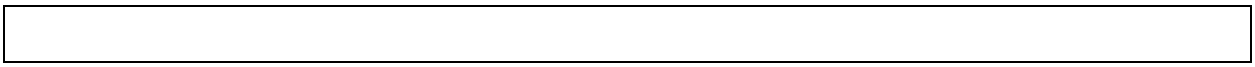

Figure 5: Variation with time (in day) of the pore solution pH of conditioning matrices, activated slag (AS), ordinary Portland cement (OPC), calcium sulfoaluminate cement (CSA), magnesium phosphate cement (MPC) and brushite cement (BC).

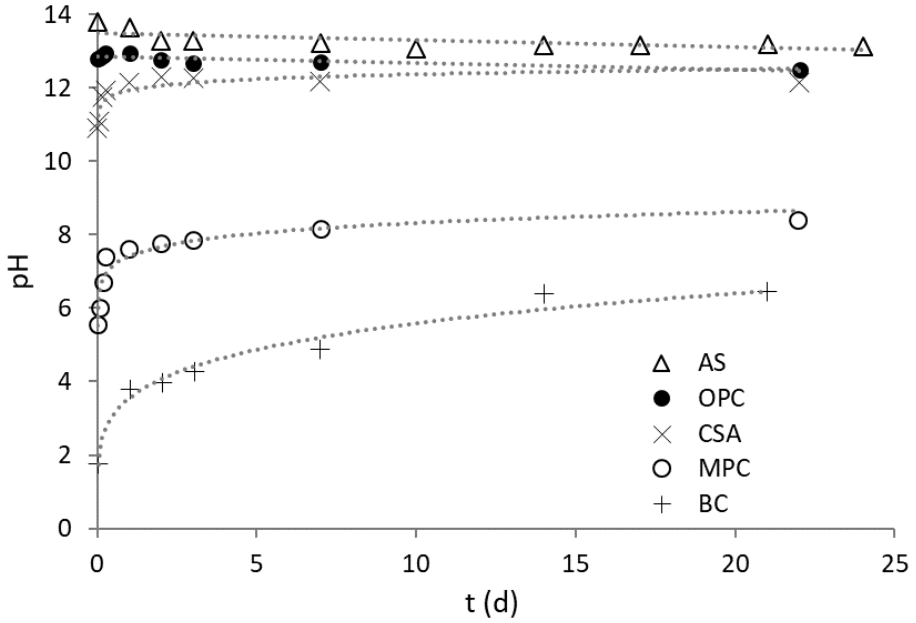

Figure 6: Superimposition of the pH domains of the selected conditioning matrices and the pH domains of the $Be(OH)_2$ stability determined in the reference [31] (grey lines) and in this work (black lines).

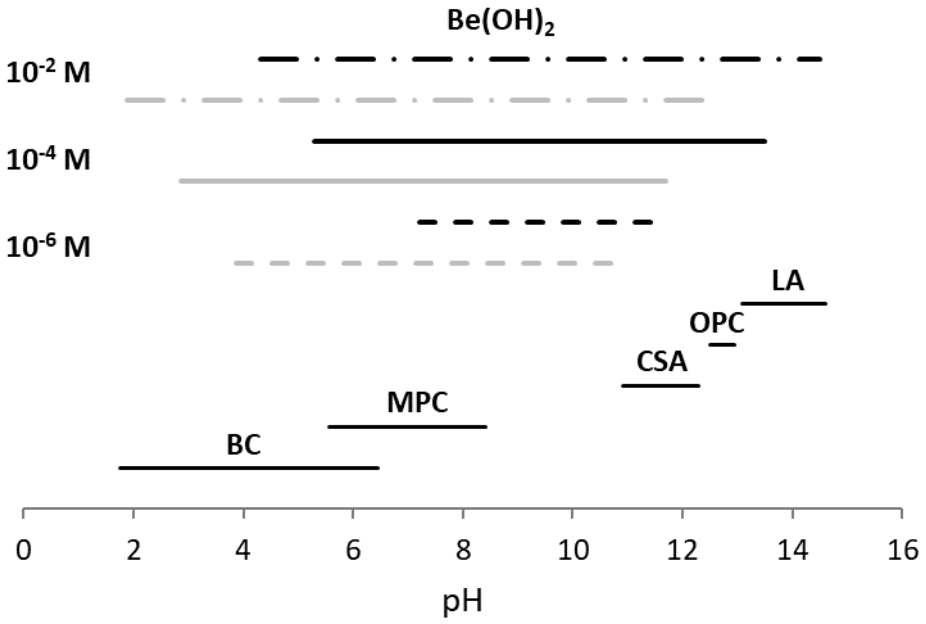

Figure 7: Comparison of the variation of the beryllium Open Circuit Potential (OCP) and the potential of the H_2O/H_2 redox couple with time (in day) in the ordinary Portland cement (OPC), calcium sulfoaluminate cement (CSA), magnesium phosphate cement (MPC), activated slag (AS) and brushite cement (BC).

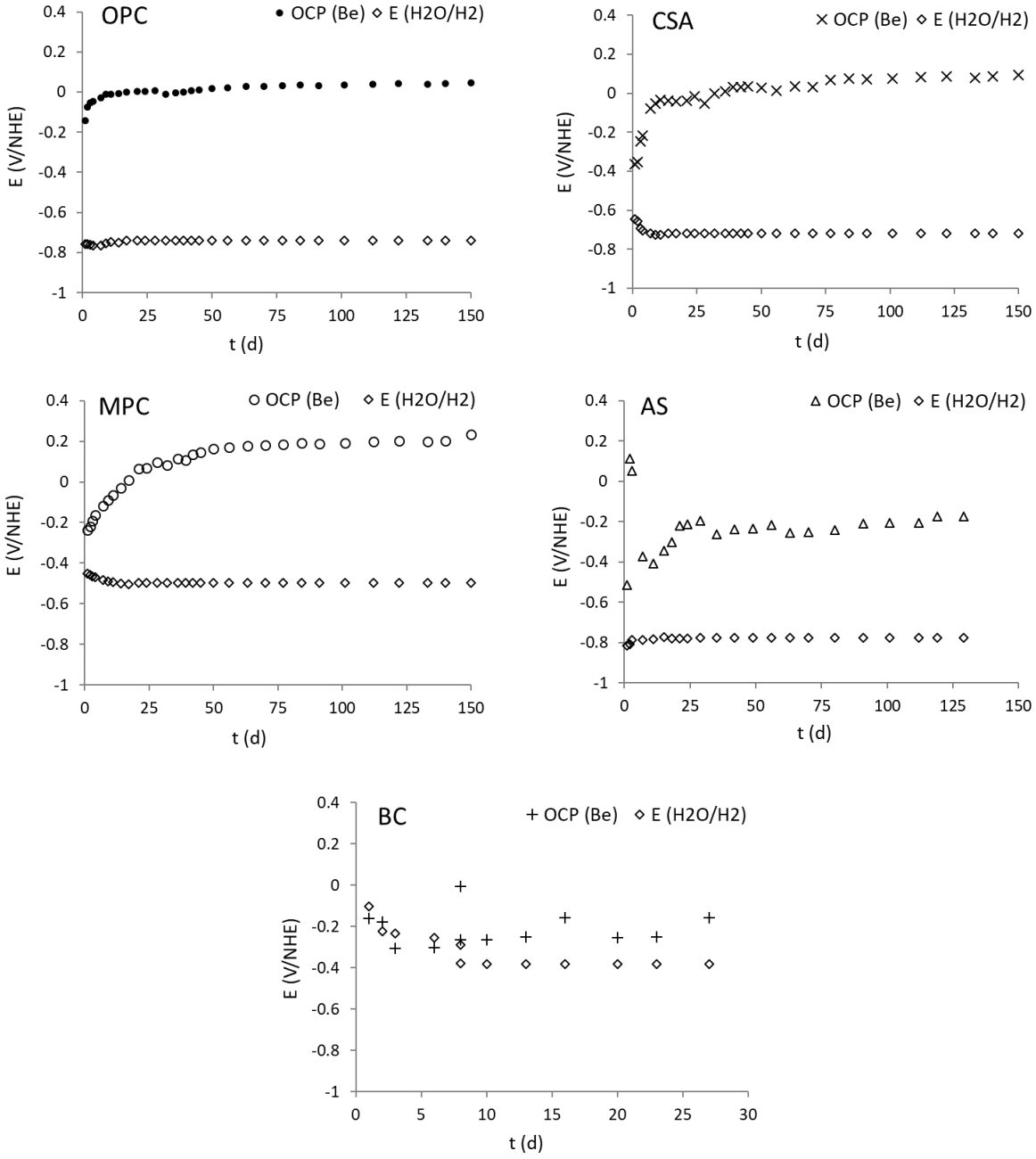

Figure 8: Variation of the difference between the beryllium OCP and the H_2O/H_2 redox potential measured in the five types of cement as a function of time (in day).

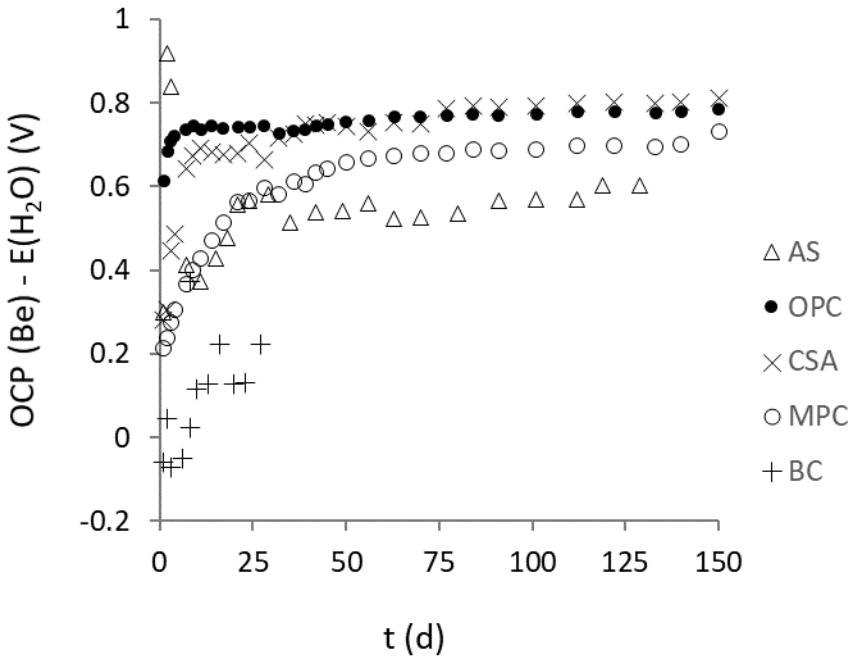

Figure 9: Electrical circuit to model the electrochemical impedance spectra.

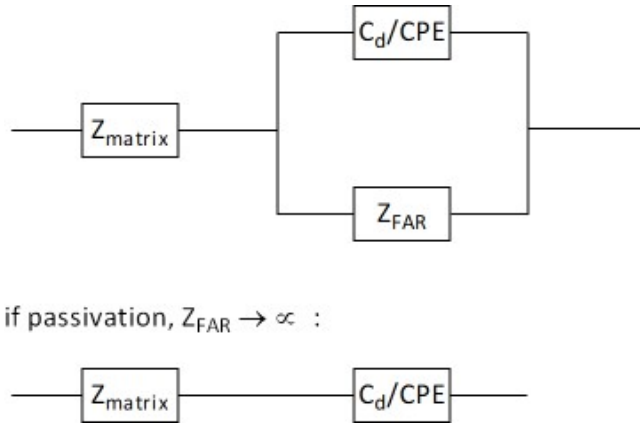

Figure 10: Electrochemical impedance diagrams (Nyquist (left) and Bode (right) representation) of a platinum electrode immersed during 7 and 101 days in ordinary Portland cement (OPC), calcium sulfoaluminate cement (CSA), magnesium phosphate cement (MPC) and activated slag (AS).

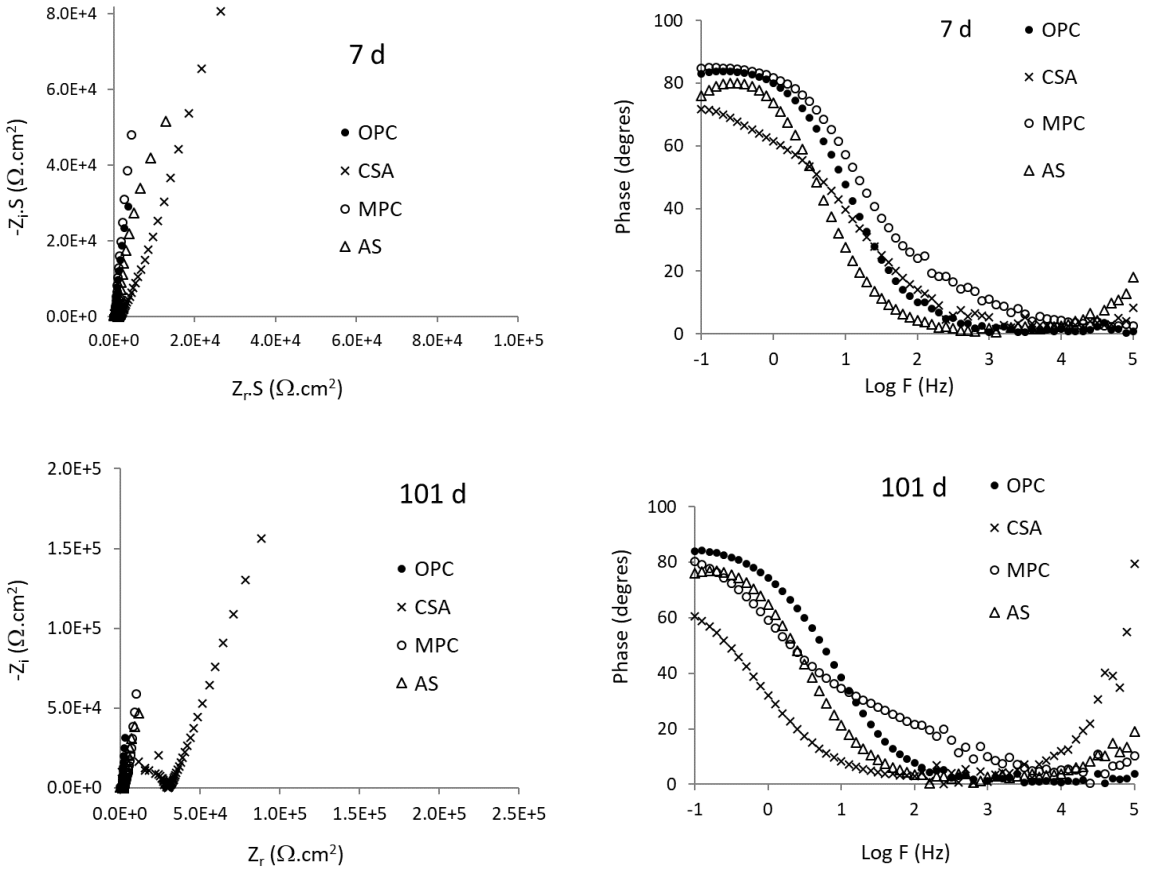

Figure 11: Electrochemical impedance diagrams (Nyquist (left) and Bode (right) representations) recorded on a beryllium electrode at the OCP, with a 10 mV amplitude, in brushite cement (BC) for different immersion times (in day).

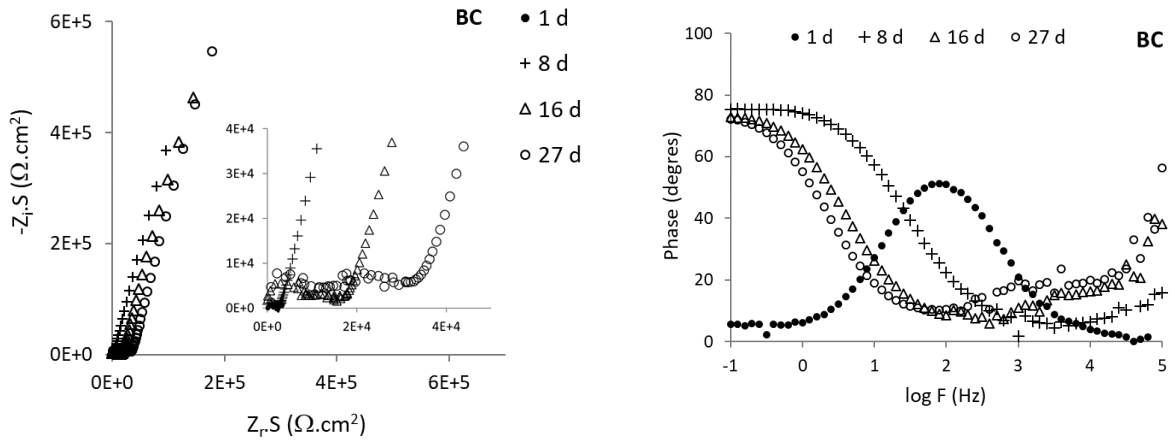

Figure 12: Electrochemical impedance diagrams (Nyquist (left) and Bode (right) representation) of a beryllium electrode immersed during different times (in day) in ordinary Portland cement (OPC), magnesium phosphate cement (MPC), activated slag (AS) and calcium sulfoaluminate cement (CSA), recorded at the OCP with a 10 mV amplitude.